Highlights on Spanish Astrophysics X, Proceedings of the XIII Scientific Meeting of the Spanish Astronomical Society held on July 16 – 20, 2018, in Salamanca, Spain. B. Montesinos, A. Asensio Ramos, F. Buitrago, R. Schödel, E. Villaver, S. Pérez-Hoyos, I. Ordóñez-Etxeberria (eds.), 2019

Low-mass planets around low-mass stars: Highlights from the HADES survey.

J. Maldonado[1]

[1] INAF - Osservatorio Astronomico di Palermo, Piazza del Parlamento 1, 90134 Palermo, Italy, e-mail:jesus.maldonado@inaf.it

Abstract

While most of the planets discovered so far have been found orbiting around solar-type stars, low-mass stars have recently been recognised as a “shortcut” to glance into an exo-life laboratory. The HArps-N red Dwarf Exoplanet Survey (HADES) program is a long-term project at the Telescopio Nazionale Galileo aimed to the monitoring of nearby, early-type, M dwarfs, using the HARPS-N spectrograph to search for small, rocky planets. In this contribution we present a summary of the project status, our methodology to determine accurate stellar parameters for these stars, as well as our efforts to understand magnetic activity in M dwarfs taking advantage of the high-quality HARPS-N spectra.

1 Introduction

Low-mass stars (M dwarfs) are nowadays recognised as promising targets in the search for rocky, small planets with the potential capabilities of supporting life [8, 24]. The HArps-N red Dwarf Exoplanet Survey (HADES) [2] is an radial velocity survey for low-mass planets around a sample of northern-hemisphere early-M dwarfs. HADES constitutes a collaborative effort between the Italian Global Architecture of Planetary Systems project (GAPS)[1] [7], the Institut de Ciències de l'Espai (ICE/CSIC), and the Instituto de Astrofísica de Canarias (IAC).

Up to date, seventy-one nearby, bright (V < 12 mag) stars have been observed. They have effective temperatures ranging from 3400 to 3900 K, with spectral types between K7.5 and M3V. Our targets were selected from the Palomar-Michigan State University (PMSU) catalogue [22], from [12], and are targets observed with the APACHE transit survey [24] and with an expected high number of *Gaia* mission scans.

High-resolution échelle spectra of the stars were obtained at La Palma observatory (Canary Islands, Spain) during several observing runs (from September 2012) using the HARPS-

[1]http://www.oact.inaf.it/exoit/EXO-IT/Projects/Entries/2011/12/27_GAPS.html

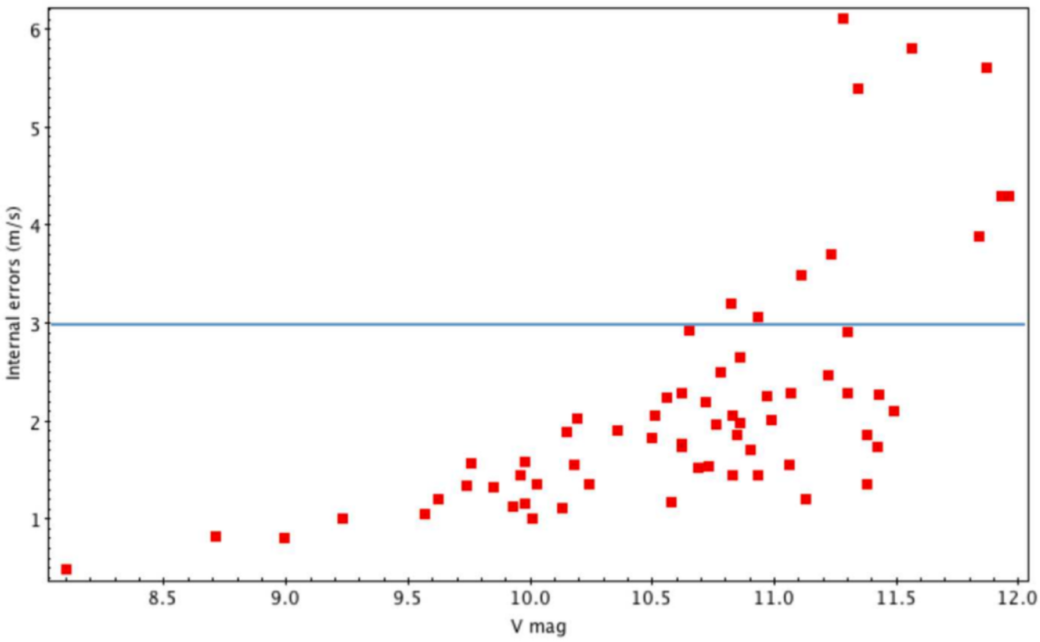

Figure 1: Radial velocity precision vs V magnitude for series of 15 min HARPS-N spectra of M dwarfs.

N instrument [6] at the Telescopio Nazionale Galileo (TNG). HARPS-N spectra cover the wavelength range 383-693 nm with a resolving power of R $\sim$ 115000. Spectra were automatically reduced using the Data Reduction Software (DRS) [13]. The DRS calculates the cross-correlation function, which is the correlation of the spectrum with an M2-type template mask in velocity space. However, we decided not to use the radial velocities determined by the DRS, but to use the Java-based Template-Enhanced Radial velocity Re-analysis Application (TERRA) [3] as we found it to deliver more accurate radial velocities in the case of M-type stars [18]. Figure 1 shows the achieved radial velocity precision as a function of the V magnitude of the stars for series of 15 minutes of exposure time. It can be seen that a radial velocity precision of the order of 1 ms^{-1} is achieved for stars with V $\sim$ 10.

2 The survey results

At the time of written, five new planets have been discovered within the HADES survey while one previously known planet has been confirmed.

GJ 3998b,c [2]. The radial velocity analysis of the M1 star GJ 3998 showed four significant signals at 30.7, 13.7, 42.5, and 2.65 days. We used state of the art techniques to disentangle keplerian from stellar signals including the analysis of optical activity indicators (Ca II H & K lines, Hα), photometry (APACHE [24], and EXORAP at INAF-Catania Astrophysical Observatory), and gaussian process analysis. An example is shown in Fig. 2 where

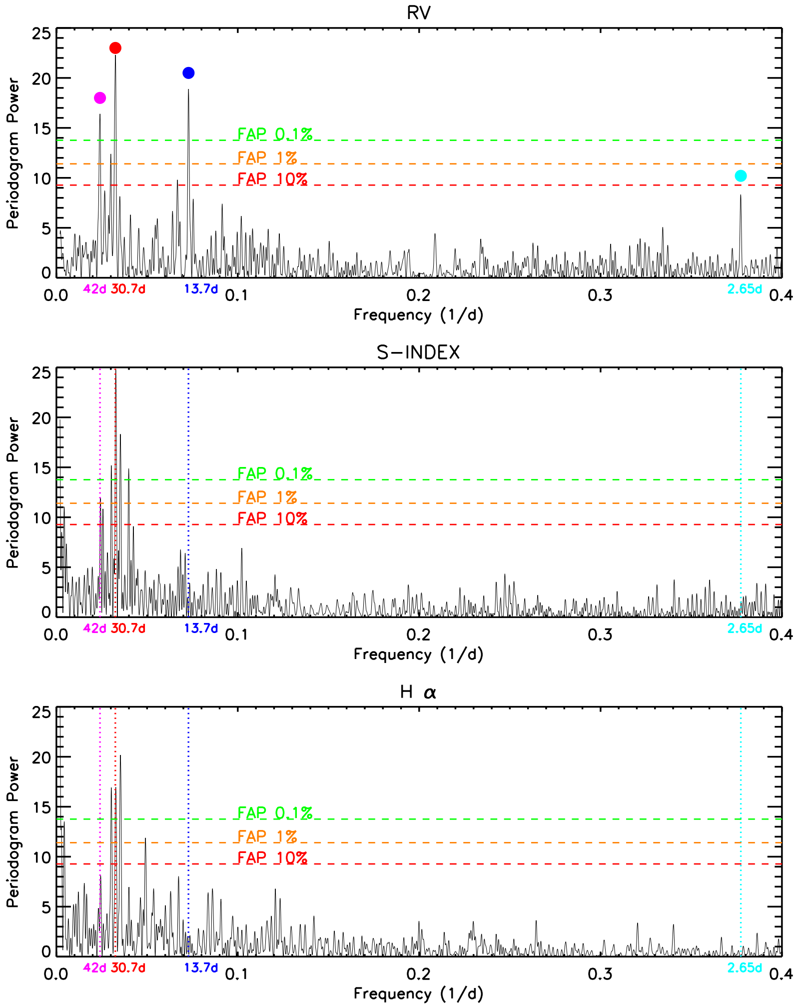

Figure 2: From top to bottom: Generalised Lomb-Scargle periodogram of radial velocities, Ca II H & K index, and Hα index for the star GJ 3998, zoomed around the frequencies of interest. The dotted blue and cyan lines indicate the frequencies corresponding to orbital periods of the candidate planets at 13.7 and 2.65 days, respectively, while the dotted red and magenta lines show the frequencies corresponding to the activity periods at 30.7 and 42.5 days, respectively. Figure taken from [2].

we show the use of activity indicators. We identified the periods of 30.7 and 42.5 days as the result of chromospheric inhomogeneities modulated by stellar and differential rotation, respectively. The shorter periods are well explained with the presence of two super-Earth like planets (GJ 3998b: P=13.74 ± 0.02 days, $m_C \sin i = 6.26 \pm 0.79\ M_\oplus$, a = 0.089 au; GJ 3998c: P=2.6498 ± 0.0008 days, $m_C \sin i = 2.47 \pm 0.27\ M_\oplus$, a = 0.029 au).

GJ 625b [26]. A super-Earth orbiting at the inner edge of the habitable zone of the star GJ 625 was discovered from the analysis of our HARPS-N radial-velocity time series. The characteristics of GJ 625b are $m_C \sin i = 2.82 \pm 0.51\ M_\oplus$ with an orbital period of 14.628 ± 0.013 days at a distance of 0.078 au. A second radial-velocity signal in the range 74-85 days was related to stellar rotation after the analysis of optical activity indicators, cross-correlation function asymmetry diagnostics and photometry light curves.

GJ 3942b [17]. By analysing five years of observations of this star we identified the rotation period of GJ 3942 at 16.3 days and discovered a new super-Earth, GJ 3942b, with an orbital period of 6.9 days and a minimum mass of 7.1 $M_\oplus$. An additional signal in the periodogram of the residuals was found. If confirmed, this planet candidate would have a minimum mass of 6.3 $M_\oplus$ and a period of 10.4 days.

GJ 15Ab,c [19]. Twenty years of radial velocity measurements of the M1 dwarf GJ 15A were analysed by combining our HARPS-N data with 15 years of archival HIRES/Keck data. We confirmed the keplerian nature of the 11.44 days period super Earth GJ 15Ab ($m_C \sin i = 3.03\ ^{+0.27}_{-0.44}\ M_\oplus$) and discovered a second long-period (76000 days) super-Neptune mass planet ($m_C \sin i = 36\ ^{+25}_{-18}\ M_\oplus$). Our best fits to the radial velocity data of GJ 15A are shown in Fig. 3.

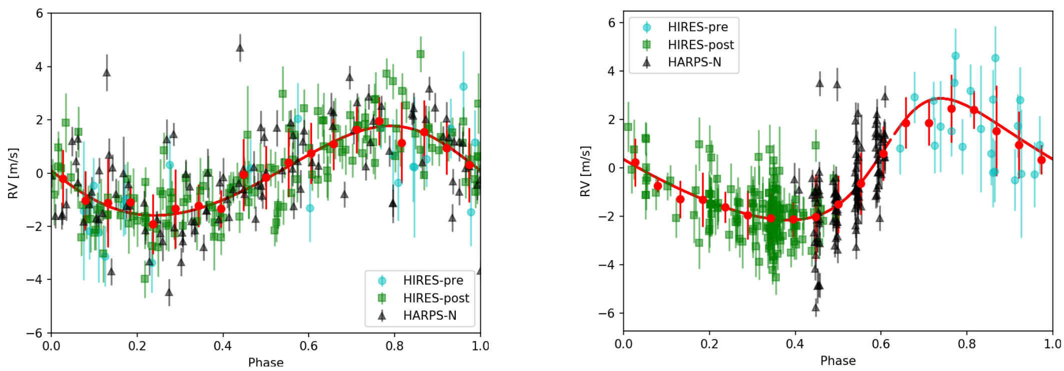

Figure 3: Phase folded radial velocity curves for GJ 15Ab (left) and GJ 15Ac (right). Each curve shows the residuals after the subtraction of the other planet and the stellar correlated signal. The red curve represents the best-fit keplerian orbit, while the red dots and error bars represent the binned averages and standard deviations of the radial velocities. Figure taken from [19].

Figure 4 summarises the HADES discoveries up to now. It can be seen that our discoveries are located in the lower part of the (minimum) mass vs period diagram of known planets around M-dwarfs. The HADES planets are mainly super-Earth like planets with minimum masses in the range 2-7 $M_\oplus$ and typical periods around 10 days. Figure 4 points

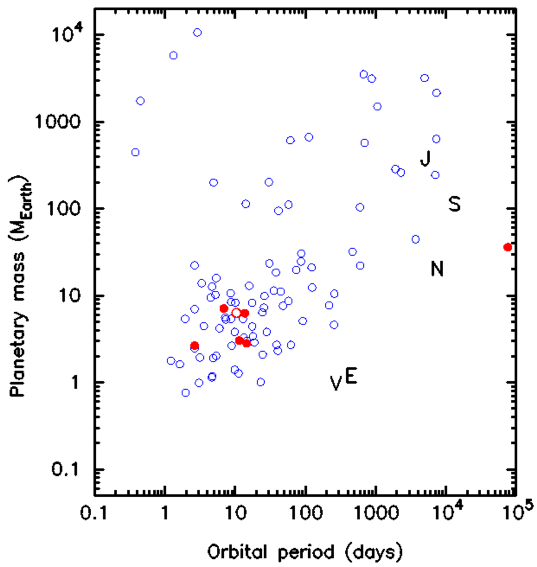

Figure 4: Known planets around M dwarfs. Data is from http://exoplanet.eu. Filled red circles indicate the HADES discoveries while candidates are shown in open circles. For comparison, the position of several Solar System planets, namely Venus, Earth, Jupiter, Saturn, and Neptune is indicated with the labels V, E, J, S, and N, respectively.

out that most planets orbiting around M dwarfs are super-Earth planets while there seems to be a lack of massive planets in close-in orbits orbiting M dwarfs.

3 Characterising the nearby early-M dwarf population

In contrast to solar type stars, the stellar parameters of M dwarfs are in general not well understood. Few M dwarfs are bright enough for a direct measurement of their radii and, in addition, there are disagreements between observations and theoretical models: observations show that M dwarfs are cooler and larger than expected.

Within HADES we have developed a technique to calibrate empirical relationships in order to determine the stellar parameters of early M-dwarfs [15]. Our methodology is based on the use of pseudo-equivalent widths of features measured in the optical spectra. A feature can be a line or a blend of lines. Pseudo-equivalent widths are defined as "traditional" equivalent-widths but measured with respect to the value of the flux between the peaks of the feature at each wavelength.

We have identified and calibrated 112 temperature sensitive ratios of features using as calibrators a sample of early M-dwarfs with angular sizes obtained with long-baseline interferometry. Typical uncertainties in our derived T_{eff} are about 70 K. Figure 5 shows same examples of ratios of features found to be sensitive to T_{eff}. In a similar way, 82 spectral-type sensitive ratios with a standard deviation lower than 0.5 spectral subtypes were identified. For metallicity, we searched for empirical relationships as a function of individual features

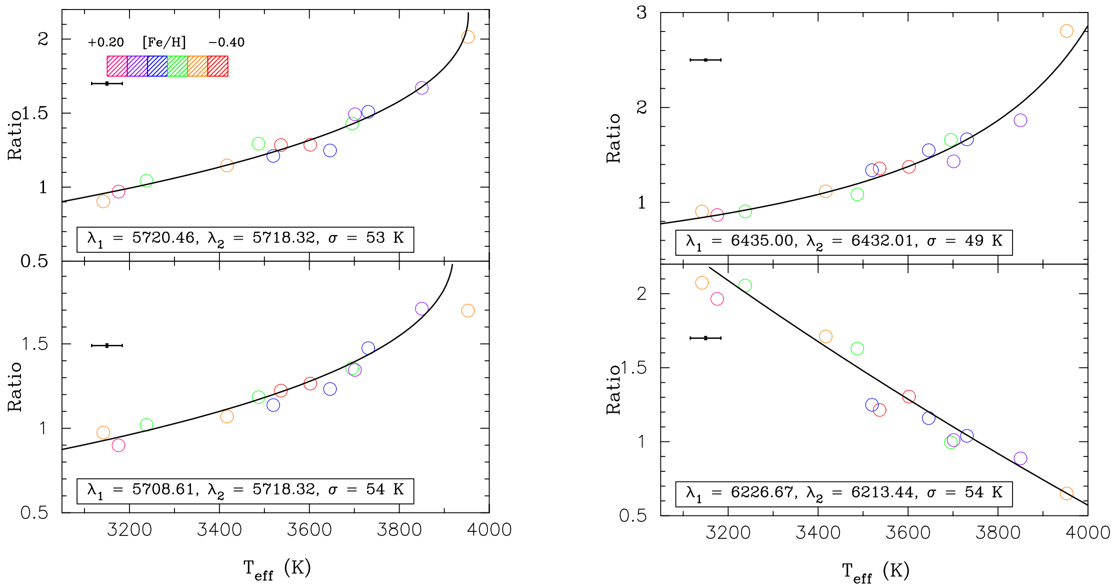

Figure 5: Examples of ratios of some features identified to be sensitive to T_{eff} in early-M dwarfs. Stars are plotted using different colours according to their metallicity. The corresponding fits are shown. The features' central wavelengths as well as the rms standard deviation of the residuals are given in each plot. Figure taken from [15].

and T_{eff}-sensitive ratios. A total of 696 calibrations with standard deviation values between 0.07 and 0.10 dex were identified. Finally, we made use of our temperature and metallicity values to search for empirical relationships with the stellar evolutionary parameters (mass, radii, $\log g$, luminosity). Our codes are public available for the community[2].

Other HADES studies have focused on understanding the chromospheres of M dwarfs. This is crucial for the HADES objectives. Stellar activity, including stellar spots, oscillations, and granulation are challenging the detection of low-mass planets via radial velocity. Further, the high-levels of activity (strong flares and high UV emission in quiescence) of M dwarfs may constitute a potential hazard for habitability.

In [14] the stellar parameters-activity relationships for early-M dwarfs were revisited. To do that, we first determine the emission excess in the different chromospheric indicators (Ca II H & K, Balmer's lines) by applying the spectral subtraction technique which allow us to subtract the underlying photospheric contribution from the stellar spectrum. We also computed rotational velocities by using the cross-correlation function and estimate the age of the stars by analysing their spatial Galactic velocity components and possible membership to stellar kinematic groups. Our results are summarised as follows: i) the strength of the chromospheric emission is constant in the M0-M3 spectral range; ii) we find lower rotation levels in cooler stars; iii) a tendency of higher rotation values with increasing activity is found; and iv) young stars tend to show higher levels of activity.

[2]https://github.com/jesusmaldonadoprado/mdslines

Figure 6 shows some examples of the comparison between pairs of fluxes of different chromospheric lines and coronal X-ray emission for the stars in our sample. The analysis of the flux-flux relationships shows that our M dwarfs sample is complementary to other literature samples, extending the analysis of the flux-flux relationships to the low-chromospheric fluxes domain. Our results confirm that field stars deviating from the "general" flux-flux relationships are likely to be young. We conclude that our sample represents a benchmark for the characterisation of magnetic activity at low levels.

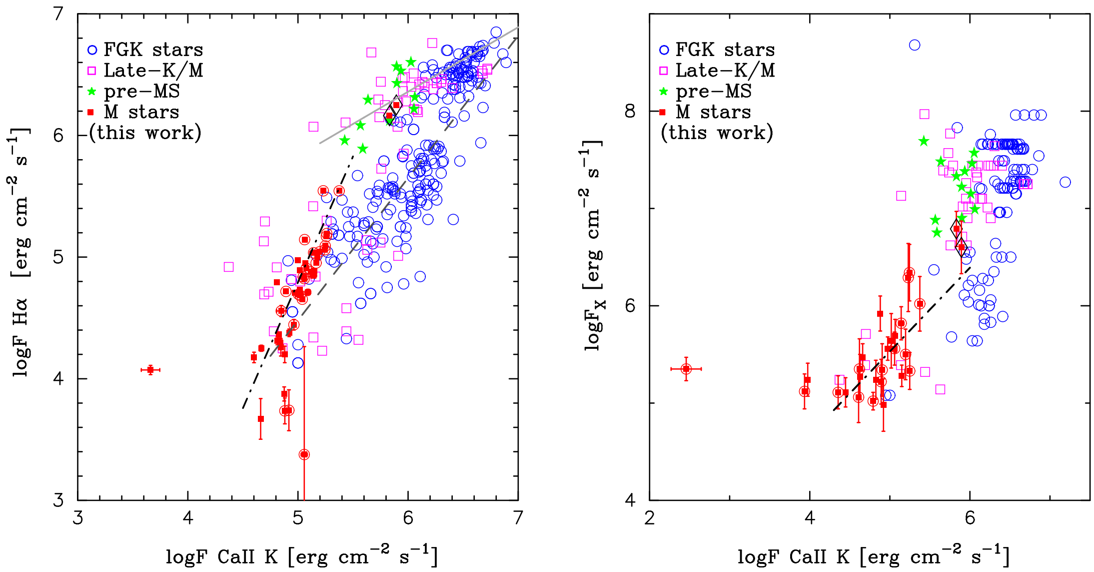

Figure 6: Flux-flux relationships between between Hα and Ca II K (left panel) and between X-ray and the calcium line Ca II K (right panel). M dwarfs from the HADES survey are plotted with red filled squares; FGK stars from the literature with open circles, late-K and M stars from the literature are shown by purple open squares; green stars denote M0-M3 pre-MS M stars. Possible young disc stars in our M star sample are shown by circles. The black dash-dotted line represents our best fit; the relations for the "active" and "inactive" branches by [16] are shown in light grey solid and dashed dark grey lines, respectively. Two "deviating" stars are indicated by diamonds. Figure taken from [14].

The short term variability of our targets is analysed in detail in [23]. The time variability of the emission fluxes is analysed by using the pooled variance technique. We derive a tentative estimate of the rotation period (on the order of a few tens of days) for some HADES targets, while we found the typical lifetime of chromospheric active regions to be of the order of a few stellar rotations. A couple of examples are shown in Fig. 7. We also find that the variance of the flux excess is an increasing function of stellar activity, and that even the quietest stars show some degree of variability.

We also find that the Hα emission does not increase monotonically with the Ca II H & K line flux, showing some absorption before being filled in by chromospheric emission when Ca II H & K activity increases, in agreement with chromospheric models.

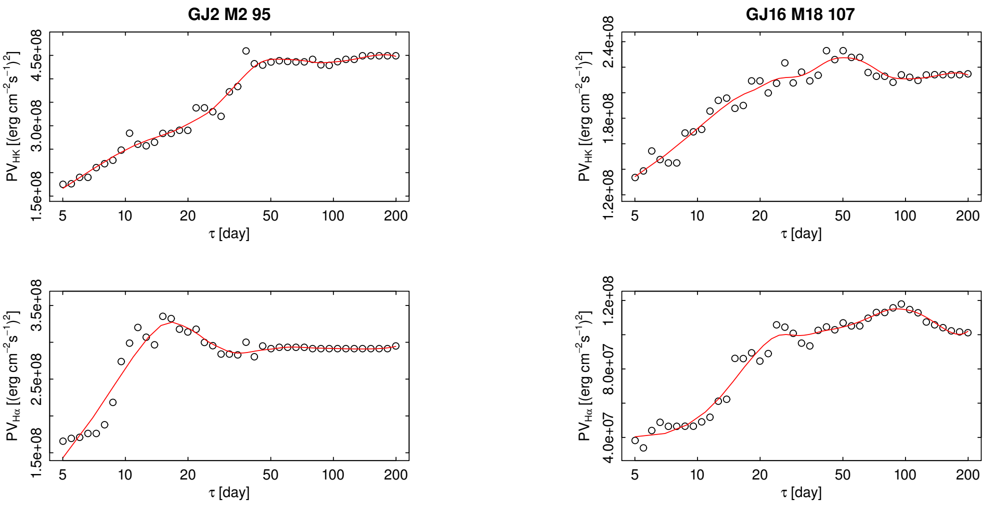

Figure 7: Pooled variance diagrams of the star GJ 2 (left) and GJ 16 (right). Top: Ca II H & K. Bottom: Hα. The red line is a smoothing function for ease of reading the graphs. Figure taken from [23].

We finally revisited the activity-rotation relationship, previously poorly constrained for M dwarfs (specially in the non-saturated regime). In [25] $\log R'_{\rm HK}$ values and rotational periods are derived from time series spectroscopy of the Ca II H & K and Hα activity indicators. Complementary ASAS photometry light-curves are also used. The typical level of activity in our sample is $\log R'_{\rm HK} \sim$ -5 while the mean rotation period of our stars is $\sim$ 40 days. The rotation-activity diagram is shown in the left panel of Fig. 8. The data is fitted to a relationship with the functional form $\log(P_{\rm rot}) = A + B \times \log R'_{\rm HK}$ being A = -2.15 and B = -0.731 for our early-M dwarfs.

The coronal activity-rotation relationship is analysed in [10]. It is important to note that all our targets except one are in the non-saturated regime where only one data point (that, in addition, corresponds to an upper limit) was reported in previous works [20]. Therefore, we are able to determine in a more accurate way than in previous works the value of the rotation period at which the saturation occurs ($P_{\rm sat}$) for M dwarfs. Figure 8, right, shows the fractional X-ray luminosity of the stars a function as a function of the period. From our analysis we derive $P_{\rm sat} \sim$ 9.6 days for stars in the 3400-3600 K range, while for stars with effective temperatures between 3700 and 3900 K the derived $P_{\rm sat}$ value is of the order of 4.4 days.

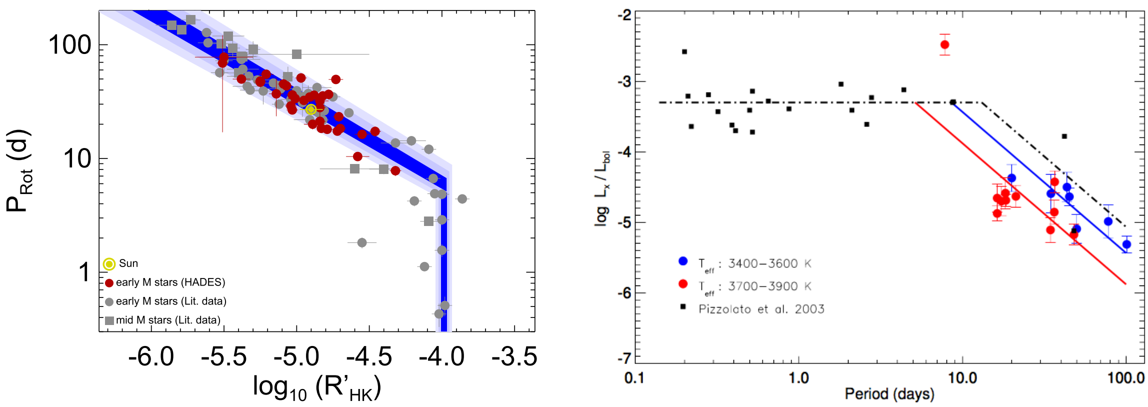

Figure 8: Left: Rotation period vs. chromospheric activity level, $\log R'_{\rm HK}$. The shaded region shows our best fit. HADES targets are shown in red, while literature data is plotted in grey. The Sun's value is included as a reference point. Figure taken from [25]. Right: L_X/L_{Bol} vs. rotation period. The black squares correspond to the upper limits from [20]. Blue and red dots correspond to the M dwarfs from this work in the two different range of temperatures indicated in the text. The black dashed line represents the broken power law obtained by the fitting procedure from [20]. The blue and red dash line represent our best fit for 3400-3600 K and 3700-3800 K $T_{\rm eff}$ range, respectively. Figure taken from [10].

4 Statistical analysis

While detailed statistical analysis are still on preparation, not far after the beginning of our survey we performed a series of simulations using state of the art planet occurrence statistics in order to define the "optimal" strategy (number of targets, number of observations, exposure time, etc.) for our survey [18]. In particular, we estimated a jitter of 2.3 ms^{-1} for our targets and compared the radial velocities as derived from the DRS with those provided by the TERRA pipeline (see Sect. 1). Our analysis showed that the TERRA radial velocities give lower rms values and should be preferred.

We analysed how the number of detected planets depends on the number of observations per star and the number of observed targets. The results can be seen in Fig. 9. Based on our analysis we expected (underestimated) the discovery of 2.4 $\pm$ 1.5 planets which is half the number of planets detected so far. We found that planets with $m_C > 2$ M$_\oplus$, $K > 2$ ms^{-1} and orbital periods between 10 and 25 days should be easily detected. We conclude that optimal results are obtained for approximately 50 observations per star with exposure times of 900 s and precision of approximately 1 ms^{-1}.

5 Summary

The HADES survey has been successful in the discovery of five new super-Earth like planets with periods around 10 days. These discoveries have been possible thanks to the development

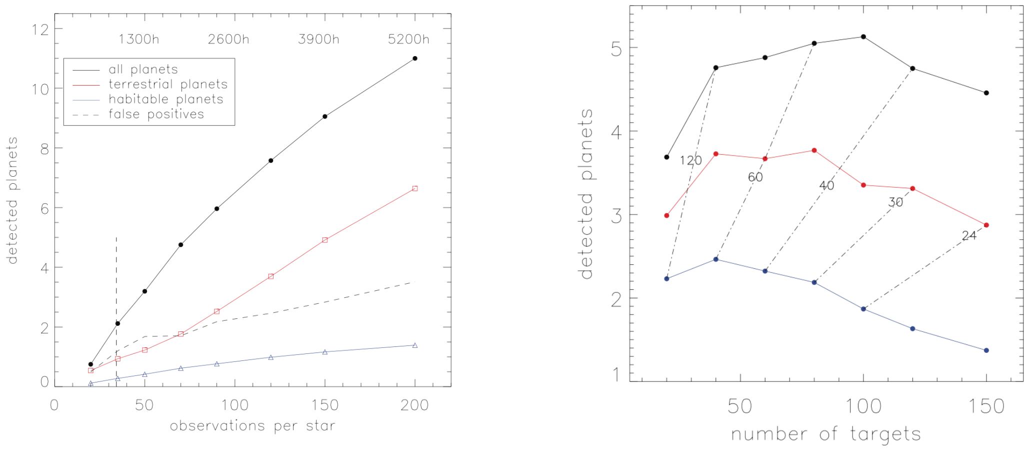

Figure 9: Left: Relationship between the amount of all detected planets and the number of observations per star (black dots), of the terrestrial planets (red squares), the habitable planets (blue triangles) and the false positives (black dashed line). The vertical black dashed line indicates the total observation time of our survey. Right: Relationship between the number of detected planets of our simulations and the number of stars used for the survey for a given total observation time of 800 (blue), 1200 (red) and 1600 h (black). Points with the same number of observations per star are connected using dash-dotted lines. Figure taken from [18].

of new and imaginative approaches to deal with the stellar noise problem. The survey is already ongoing and the analysis of the data has revealed several planetary candidates that will be the subject of further studies [1, 9].

Within HADES we have conducted several studies in order to characterise the nearby, early-M dwarf population. In particular we have analysed their stellar parameters, the relationship between them an stellar activity, the flux-flux relationships and the rotation-activity connection. In addition, several statistical analysis has been performed (regarding the survey strategy and expectations) or are in progress (including the survey sensitivity and frequency of planets, possible correlations with stellar properties, activity and binaries studies, etc.).

We finally mention the possible synergies with other projects, in particular with the development of near infrared high-resolution spectrographs like GIARPS [5] or CARMENES [21]. We note that the capabilities of combined optical/near infrared spectroscopy to confirm or reject planetary candidates have already been demonstrated [11, 4] offering an unique procedure to disentangle stellar from keplerian signals. Near infrared spectroscopy also opens for the first time the possibility of search for planets around late-type M dwarfs (spectral type later than M3-M4) for which the velocity amplitude of a terrestrial planet in the habitable zone is highest [8].

Acknowledgments

This research was supported by the Italian Ministry of Education, University, and Research through the *PREMIALE WOW 2013* research project under grant *Ricerca di pianeti intorno a stelle di piccola massa*. Additional support from the Ariel ASI-INAF agreement N. 2015-038-R.0 is also acknowledged.

References

[1] Affer L., et al., 2018, A&A, in prep.

[2] Affer L., et al., 2016, A&A, 593, A117

[3] Anglada-Escudé G., Butler R. P., 2012, ApJS, 200, 15

[4] Carleo I., et al., 2018, A&A, 613, A50

[5] Claudi R., et al., 2017, EPJP, 132, 364

[6] Cosentino R., et al., 2012, SPIE, 8446, 84461V

[7] Covino E., et al., 2013, A&A, 554, A28

[8] Dressing C. D., Charbonneau D., 2013, ApJ, 767, 95

[9] Garrido Rubio, A., et al., 2018, A&A, in prep.

[10] González-Álvarez E., et al., 2018, A&A, in prep.

[11] González-Álvarez E., et al., 2017, A&A, 606, A51

[12] Lépine S., Gaidos E., 2011, AJ, 142, 138

[13] Lovis C., Pepe F., 2007, A&A, 468, 1115

[14] Maldonado J., et al., 2017, A&A, 598, A27

[15] Maldonado J., et al., 2015, A&A, 577, A132

[16] Martínez-Arnáiz R., López-Santiago J., Crespo-Chacón I., Montes D., 2011, MNRAS, 414, 2629

[17] Perger M., et al., 2017, A&A, 608, A63

[18] Perger M., et al., 2017, A&A, 598, A26

[19] Pinamonti M., et al., 2018, arXiv, arXiv:1804.03476

[20] Pizzolato N., Maggio A., Micela G., Sciortino S., Ventura P., 2003, A&A, 397, 147

[21] Quirrenbach A., et al., 2014, SPIE, 9147, 91471F

[22] Reid I. N., Hawley S. L., Gizis J. E., 1995, AJ, 110, 1838

[23] Scandariato G., et al., 2017, A&A, 598, A28

[24] Sozzetti A., et al., 2013, EPJWC, 47, 03006

[25] Suárez Mascareño A., et al., 2018, A&A, 612, A89

[26] Suárez Mascareño A., et al., 2017, A&A, 605, A92